CHINESE OPTICS LETTERS

Vol. 19, No. 8 | August 2021

Real-time and ultrafast optical pulse quantization based on slicing the supercontinuum

Ya Guo (郭 亚)[1,4,†], Qiang Cai (蔡 强)[1,†], Zhiwei Jia (贾志伟)[1], Bingjie Xu (徐兵杰)[5], Zhensen Gao (高震森)[2], Qianwu Zhang (张倩武)[3], Ruonan Zhang (张若南)[4], Adonis Bogris[6], K. Alan Shore[7], Yuncai Wang (王云才)[2], and Pu Li (李 璞)[1,2,3*]

[1] Key Laboratory of Advanced Transducers and Intelligent Control System, Ministry of Education, Taiyuan University of Technology, Taiyuan 030024, China

[2] School of Information Engineering, Guangdong University of Technology, Guangzhou 510006, China

[3] Key Laboratory of Specialty Fiber Optics and Optical Access Networks, Shanghai University, Shanghai 200444, China

[4] School of Electronics and Information, Northwestern Polytechnical University, Xi'an 710072, China

[5] Science and Technology on Communication Security Laboratory, Institute of Southwestern Communication, Chengdu 610041, China

[6] Department of Informatics and Computer Engineering, University of West Attica, Athens 12243, Greece

[7] School of Electronic Engineering, Bangor University, Wales LL57 1UT, United Kingdom

*Corresponding author: lipu8603@126.com

Received September 7, 2020 | Accepted December 30, 2020 | Posted Online April 19, 2021

All-optical analog-to-digital conversion is a paramount issue in modern science. How to implement real-time and ultrafast quantization to optical pulses with different intensities in an all-optical domain is a central problem. Here, we report a real-time demonstration of an all-optical quantization scheme based on slicing the supercontinuum in a nonlinear fiber. In comparison with previous schemes through off-line analysis of the power of different optical spectral components in the supercontinuum, this, to the best of our knowledge, is the first demonstration of such functionality online in the time domain. Moreover, the extinction ratio among the quantized outputs can exceed 10 dB, which further confirms the feasibility of the proposed quantization scheme. The current 3 bit resolution in the proof-of-principle experiment is limited by the current experimental condition, but it can be expected to be greatly enhanced through improving both the spectral width of the generated supercontinuum and the number of filtering channels used.

Keywords: all-optical analog-to-digital conversion; photonic quantization; all-optical signal processing; supercontinuum generation.

DOI: 10.3788/COL202119.081901

1. Introduction

All-optical analog-to-digital converters (ADCs) have great potential applications in the fields of optical communication, satellite navigation, medical imaging, and electronic reconnaissance[1–4]. Especially, all-optical ADCs will play the critical role of converting continuous-time analog signals into discrete-time digital forms for next generation communication in the future, where all signal processing is required to be done in the all optical domain[5].

With the development of mode-locked lasers (MLLs), various outstanding photonic ADCs have been reported (a useful overview can be found in Ref. [6]). However, their quantization procedures in nearly all photonic ADCs are mainly achieved in the electrical domain. Generally speaking, their optically sampled high-speed pulse sequences need to be further demultiplexed in the time or wavelength domain into several relatively low rate electrical signals and then quantized by traditional electronic quantizers such as comparators. Consequently, the implementation of real-time and ultrafast quantization in the all-optical domain (without optoelectronic conversion) is still a central problem.

Targeting this issue, several 'all-optical' quantization techniques have been proposed[7–13]. For example, our group recently reported two different all-optical quantization schemes based on phase-shift lasers[7] and nonlinear fiber ring resonators[8], respectively. Ho *et al.* realized all-optical quantization based on the spectral broadening of a weak probe (carrier) pulse by a more intense pump (signal) pulse through the cross-phase modulation (XPM) process in fibers[9]. Oda *et al.* reported an all-optical quantization scheme based on filtering the broadened and split spectrum induced by the soliton effect or self-phase

modulation (SPM) effect in fiber[10]. Konishi *et al.* demonstrated an all-optical quantization scheme using the soliton frequency shift (SFS) in a fiber and a pulse-shaping method[11]. Xu *et al.* developed another all-optical scheme by combing the SFS with a set of spectral filters[12]. Ikeda *et al.* presented that using nonlinear fiber Sagnac loops could realize the function of all-optical quantization[13].

However, all of the aforementioned all-optical schemes are very complicated. For instance, the XPM-based schemes require the strict synchronization of a probe pulse with a sampled pulse. When the SPM-induced schemes are adopted, their available spectrum is relatively narrow so that the central wavelength of each quantization channel must be carefully adjusted around that of the pump signal. In those schemes based on SFS, a subpicosecond optical pulse source is required to obtain sufficient frequency shifts, so the optical pulses with a width of a few picoseconds, easily obtained by commercially available MLLs, should be compressed before being used as sampled pulses.

On the other hand, we notice that slicing a supercontinuum (SC) spectrum may provide a simple method for all-optical quantization. In 2005, Oda *et al.* proposed a slicing-SC-based all-optical quantization scheme in an off-line scenario by analyzing the power of different spectral components[14]. Based on his idea, researchers reported several improved schemes in recent years[15–17]. Regrettably, nearly all of their quantization processes were demonstrated only by off-line (not real-time) optical spectral power analysis. Moreover, their quantization rate of these schemes was still at a relatively low level (MSa/s).

Here, we report a real-time realization of an all-optical quantization scheme based on slicing the SC generated in a highly nonlinear optical fiber (HNLF). In comparison with previous schemes through off-line analysis of the power of different optical spectral components in the SC, this work shows for the first time, to the best of our knowledge, that the quantization function can be implemented online in the time domain.

The proof-of-principle experimental results show that the extinction ratio among the quantized outputs can exceed 10 dB, which is compatible with current optical communication standards. Although we only give a demonstration of 10 GSa/s and 3 bit all-optical ADC in the proof-of-principle experiment that is limited by our experimental conditions, a higher quantization resolution is expected through improving the spectral width of the generated SC and the number of filtering channels used in the quantizing process. In addition, our scheme of all-optical quantization has potential to be integrated into a compact device using silicon technologies.

2. Experimental Setup and Results

Figure 1 shows the schematic of the proposed real-time all-optical quantization based on slicing the SC in an HNLF with an arrayed waveguide grating (AWG). The whole setup can basically be divided into two crucial parts: (a) sampling and (b) quantizing, as shown in Fig. 1.

In the all-optical sampling part [Fig. 1(a)], a train of picosecond optical pulses generated from an ultrafast MLL (Pritel, UOC-05-14 G-E) is injected into the electro-optical modulator (EOM, Photline, MXAN-LN-10) as the sampling optical clock. Meanwhile, a sinusoidal RF signal amplified by the electronic amplifier (AMP, SHF826h) is fed into the EOM as the sampled analog signal. Through adjusting an appropriate bias voltage of the EOM, the sinusoidal analog signal can be linearly modulated onto the sampling optical clock pulses.

Figure 2 shows the measured optical sampling results, recorded by a 36 GHz real-time oscilloscope (Lecroy, LabMaster10-36Zi) via a 45 GHz photo-detector (PD, U2TXPDV2120RA). Specifically, Fig. 2(a) is the temporal waveform of the 10 GHz MLL pulse train with a central wavelength of 1556.2 nm. Figure 2(b) depicts the sampled optical pulse train after the EOM. As is shown, the peak envelope of the output sampled pulses matched the sine wave very well, which confirms high-fidelity sampling.

Figure 1(b) illustrates the optical quantization. The optically sampled pulse sequence is firstly amplified by the Er-doped fiber AMP (EDFA, KEOPSYS, PEFA-SP-C-SM-33-B2020-FA) to an average power of 50 mW and then used to pump a 400 m HNLF to obtain the SC pulse sequence. Note, typical parameters of the

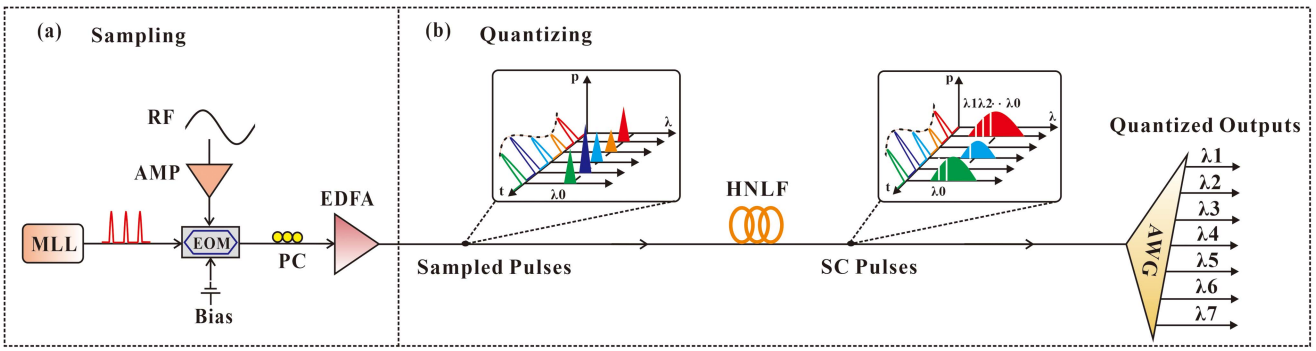

Fig. 1. Schematic diagram of the proposed post-processing-free fast quantum random number generator (QRNG) based on optically sampling ASE. SLD, superluminescent diode; EDFA, Er-doped fiber amplifier; BPF, optical band-pass filter; MLL, mode-locked laser; WDM, wavelength division multiplexer coupler; SOA, semiconductor optical amplifier; PC, polarization controller; 50:50, 50:50 optical coupler; TOAD, terahertz optical asymmetric demultiplexer; ISO, optical isolator; PD, photodetector; 8 bit quantizer, an 8 bit parallel comparator module built in a high-speed real-time serial data analyzer.

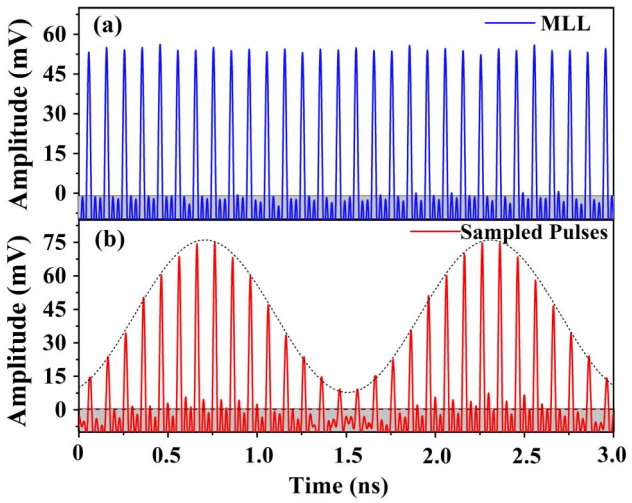

Fig. 2. Measured results of real-time optical sampling of the 625 MHz sinusoidal RF signal. (a) Temporal waveform of the 10 GHz MLL pulses out from the MLL. (b) Temporal waveform of the sampled pulses out from the EOM.

HNLF are $\gamma = 10\ \mathrm{W^{-1} \cdot km^{-1}}$, $\beta = 0.017\ \mathrm{ps \cdot nm^{-2} \cdot km^{-1}}$, and zero-dispersion wavelength (ZDW) is 1550 nm, respectively. In this process, the sampled pulses with different amplitudes will experience different spectral broadening. The spectral broadening width of the obtained SC pulse is proportional to the amplitude of the pump sampled pulse. According to this, each sampled pulse with different amplitudes can be successfully quantized by mapping the spectral broadening level.

In our experiment, we realize the quantization to the pump sampled pulses by slicing the SC spectrum using an array of filters with different transmission wavelengths. Specifically, the generated SC spectrum pulses after the array of filters are split into n independent SC pulse subsequences with different output central wavelengths from λ_1 to λ_n. Therefore, the SC pulse subsequences with the central wavelength from λ_1 to λ_n can be considered as n equivalent threshold decision outputs from a multi-bit ADC, respectively.

Similar to the electronic ADCs, the basis for our time domain code to filter channels is also the binary digital coding. As shown in Fig. 3(a), the amplitude ranges of the SC pulses to be coded need to be divided into "2^N" equal levels by means of "$2^N - 1$" filtering channels (i.e., "$2^N - 1$" decision thresholds) for an N-bit quantization. Herein, we consider a 3 bit quantization to provide a real-time demonstration of the proposed scheme. The range of the SC pulses is divided into eight strips with a quantization step of $\Delta = 10/80$ mV. Each strip from the bottom to top can be coded into "000", "001", "010", "011", "100", "101", "110", and "111", respectively.

In fact, it should be pointed that each 3 bit code corresponds to filtering output channels finally. As illustrated in Fig. 1(b), different sampled pulses with different amplitudes will experience different spectral broadening. So, we need to select seven filtering channels with appropriate wavelength intervals to guarantee

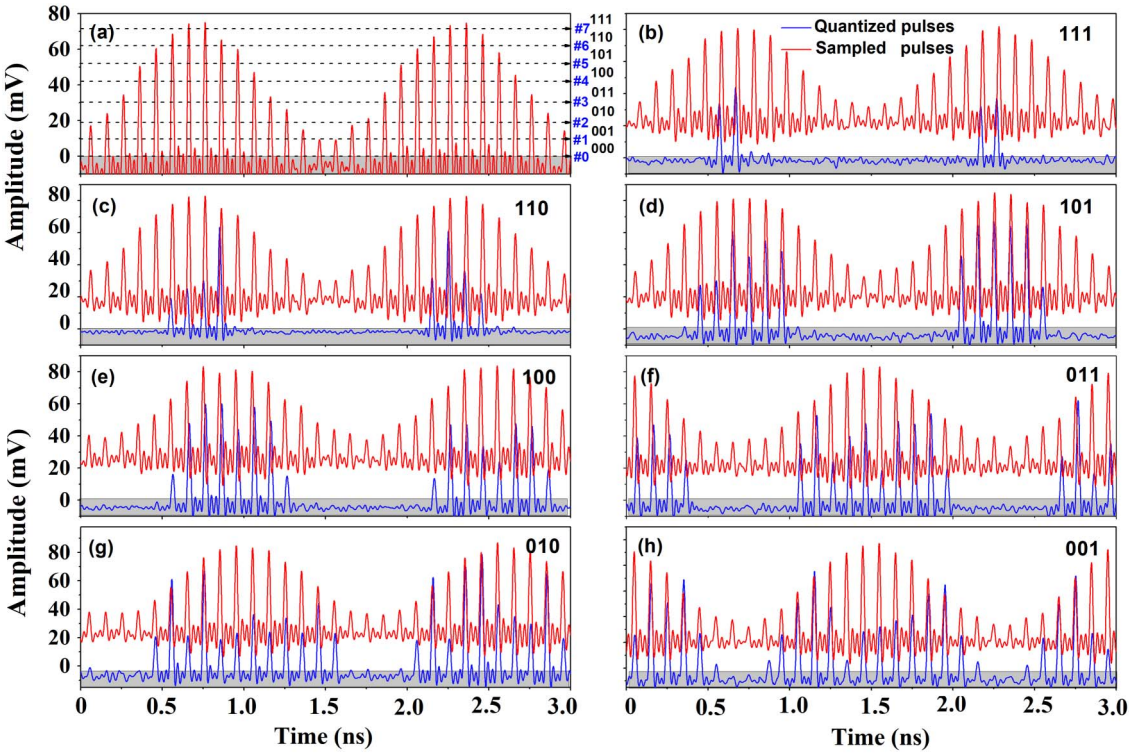

Fig. 3. Measured results of real-time all-optical quantization. (a) Temporal waveform of the sampled optical pulses to be quantized; (b)–(h) temporal waveforms (blue line) of the quantized output pulses from λ_1, λ_2, λ_3, λ_4, λ_5, λ_6, and λ_7 filtering channels, respectively. Note, red lines represent the synchronous temporal waveform of the input sampled pulses.

that only when the sampled pulse amplitude is located at the first strip from the top to the bottom can its corresponding generated SC pulse pass the #7 filtering channel with a center wavelength of λ_7. When the sampled pulse amplitude is located at the second strip from the top to the bottom, its SC pulse can pass #6 filtering channels with a center wavelength of λ_6, and so on, for each sampled pulse in the other seven strips. To realize this aim, in our proof-of-principle experiment, the 2^3-1 filtering center wavelengths with a 0.8 nm filtering bandwidth are $\lambda_1 = 1553$ nm, $\lambda_2 = 1550$ nm, $\lambda_3 = 1545$ nm, $\lambda_4 = 1541$ nm, $\lambda_5 = 1536$ nm, $\lambda_6 = 1530$ nm, and $\lambda_7 = 1526$ nm, respectively. In this situation, the sampled pulses in each strip will get correct time domain codes. In the measurement, the sampled pulses are divided into two beams by a 99:1 optical coupler: 99% is used to pump the HNLF for SC generation and subsequent quantization, whilst 1% is used as a reference path (i.e., red temporal waveforms in Fig. 3). Both beams are synchronously recorded by the multi-channel real-time oscilloscope.

To explain the quantization results more clearly, we take three middle quantization thresholds as an example. As shown in Fig. 3(e), there are 16 sinusoidal sampled pulses in each sine period (red line), but only the eight intermediate higher-amplitude sampled pulses can pass through the λ_4-filtering channel (blue line). Similarly, Fig. 3(f) shows that only 10/16 of the sampled pulses can travel through the λ_5-filtering channel. That is $6/16 = 3/8$ is the real value of this level, which corresponds to 011. Similarly, Fig. 3(g) shows that only 12/16 of the sampled pulses can travel through the λ_6-filtering channel (010). These results demonstrate the feasibility of our all-optical quantization scheme based on slicing the SC spectrum.

In addition, it should be noted that, as shown in Fig. 2 or 3(a), the weak sidelobe pulses are a noise floor below the quantized level (i.e., the dashed lines). In our experiment, the MLL (Pritel, UOC-05-14 G-E) has a high signal-to-noise ratio (SNR) about 60–70 dB. Moreover, the weak sidelobe pulses will be quickly consumed during the transmission in the HNLF. That is, the weak sidelobe pulses almost do not work in the spectrum broadening and subsequent quantizing processes. Thus, their impact on the dynamic range of the system can be expected to be negligible.

Moreover, it should be emphasized that in comparison with previous schemes through off-line analysis of the power of different optical spectral components in the SC, our work is the first, to the best of our knowledge, demonstration of such functionality online in the time domain. From Fig. 3, one can directly achieve the binary coding only according to the waveforms of the quantized outputs in the time domain. When there is a pulse output, we code it as "1"; otherwise, when there is no pulse output, we code it as "0". These results mean that our scheme can simultaneously complete real-time quantizing and encoding in the all-optical domain, with no need of any optoelectronic conversion.

Further, we use the SNR (in dB) and the effective number of bits (ENOB) to evaluate quantitatively the performance of our all-optical quantization system[6]:

$$\mathrm{SNR} = 10\log\left(\frac{P_S}{P_N}\right), \tag{1}$$

$$\mathrm{ENOB} = \frac{\mathrm{SNR} - 1.76}{6.02}. \tag{2}$$

Here, P_S and P_N are the signal and noise power without the DC component. After calculation, it can be obtained that the SNR and ENOB are 19.1 dB and 2.88 bit, respectively. The SNR of 19.1 dB means a level far above the current optical communication standard. The ENOB of 2.88 bit indicates that only 0.12 bit degradation is generated compared to an ideal 3 bit resolution, affected by the fluctuation of the pulse signal and noise. Both of them verify that our real-time quantization scheme is suitable for practical application. From the quantization result in Fig. 3, one can clearly observe that the amplitude fluctuation among the quantized output pulses is large, although a high SNR has been reached. This is caused by the uneven energy distribution of the optical spectra of the SC generation, which incoherently limits the improvement of the extinction ratio in the quantized pulses. This issue may be resolved using specially designed waveguides to generate the SC[14].

3. Discussion

Noting that in our proof-of-principle experiment, we only give a demonstration of 3 bit all-optical ADC limited by current experimental conditions. Higher quantization resolution is expected through improving two key factors: one is the spectral width of the generated SC, and the other is the number of filtering channels. From Fig. 4, one can observe that the spectral width of the SC is about 100 nm when the average optical power of the sampled pulses is 50 mW. However, limited by the available AWG, only a small part of the spectral width from 1526 to 1553 nm is utilized in the proof-of-principle experiment. If an appropriate AWG with more filtering channels is utilized, a

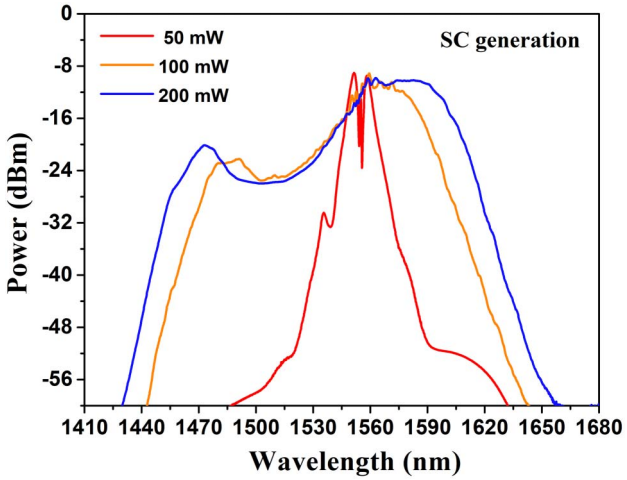

Fig. 4. Measured SCs from the 400 m HNLF with the average power of the sampled pulses increasing from 50 to 200 mW.

higher quantization resolution should be realized through employing a much wider spectrum. On the other hand, as is known, the spectral width of the generated SC depends on the input power launched into the HNLF. If the input pulse power covers a sufficiently large range, and the number of the filtering channels can be increased accordingly, the quantization resolution will be further enhanced. The spectral width of the SC can be further enhanced to roughly several hundred nanometers (nm) merely by increasing the average power of the pump pulse sequences (i.e., sampled pulses), as shown in Fig. 4. From this point of view, our method also has great potential to reach a higher quantization resolution. Note, the reason why we choose 50 mW in our current work is also limited by the filtering range of the available AWG.

In addition, we want to point out that the current experiment uses nonlinear fibers to generate SCs so that the whole all-optical quantization system is relatively bulky. However, we observe that silicon or chalcogenide waveguides have been reported with higher nonlinear coefficients and compact sizes in recent years[18,19]. If the silicon technologies are introduced to replace the nonlinear fiber in the current system, our scheme may be monolithically integrated and thereby provide a highly compact device. Our future work indeed aims to combine photonic integrated circuit technology with the proposed real-time all-optical ADC scheme in the future.

Finally, we want to include our discussion on the effective bandwidth of the system. In such a system, the analog input signal is sampled via an EOM and then quantized by slicing the SC in the HNLF. The used optical nonlinear effects in fibers have an ultra-fast response time at the femtosecond (fs) scale[20,21]. Thus, the effective bandwidth of this system is finally determined by the maximum bandwidth of the EOM used in the experiment. At present, an EOM with a modulation bandwidth of about 100 GHz has been reported[22,23]. Therefore, the effective bandwidth of our system has the potential to reach a level of 100 GHz or even higher.

4. Conclusion

In conclusion, we have proposed a 'real-time' all-optical quantizing method based on slicing the SC in HNLFs. Compared to the existing SC quantization schemes[14–16], this scheme realizes real-time on-line quantization in the time domain, with no need of any electronic processing. The proof-of-principle experiment described here demonstrated 10 GSa/s 3 bit all-optical quantization (limited by the available AWG), but high resolution is expected by increasing the pump optical power or the filtering channels. In addition, this scheme has the potential to be integrated into a compact device using silicon technologies.

Acknowledgement

This work was supported by the National Natural Science Foundation of China (NSFC) (Nos. 61775158, 61961136002, 61927811, U19A2076, 61705159, and 61805168), the National Cryptography Development Fund (No. MMJJ20170127), the China Postdoctoral Science Foundation (Nos. 2018M630283 and 2019T120197), the Natural Science Foundation of Shanxi Province (No. 201901D211116), STCSM (No. SKLSFO2018-03), the Project of Key Laboratory of Radar Imaging and Microwave Photonics (Nanjing University of Aeronautics and Astronautics), the Ministry of Education (No. RIMP2019002), and the Program for the Top Young Academic Leaders of High Learning Institutions of Shanxi.

†These authors contributed equally to this work.

References

1. A. Maruta and S. I. Oda, "Optical signal processing based on all-optical analog-to-digital conversion," Opt. Photon. News **19**, 30 (2008).
2. R. H. Walden, "Analog-to-digital converter survey and analysis," IEEE J. Sel. Areas Commun. **17**, 539 (1999).
3. F. Yang, W. W. Zou, L. Yu, S. F. Xu, and J. P. Chen, "Impact of optical-electrical conversion responsivity in sub-sampled photonic analog-to-digital converter," Chin. Opt. Lett. **17**, 040602 (2019).
4. K. J. Zheng, W. W. Zou, L. Yu, N. Qian, and J. P. Chen, "Stability optimization of channel-interleaved photonic analog-to-digital converter by extracting of dual-output photonic demultiplexing," Chin. Opt. Lett. **18**, 012502 (2020).
5. R. Slavík, F. Parmigiani, J. Kakande, C. Lundström, M. Sjödin, P. A. Andrekson, R. Weerasuriya, S. Sygletos, A. D. Ellis, L. Grüner-Nielsen, D. Jakobsen, S. Herstrøm, R. Phelan, J. O'Gorman, A. Bogris, D. Syvridis, S. Dasgupta, P. Petropoulos, and D. J. Richardson, "All-optical phase and amplitude regenerator for next-generation telecommunications systems," Nat. Photon. **4**, 690 (2010).
6. G. C. Valley, "Photonic analog-to-digital converters," Opt. Express **15**, 1955 (2007).
7. P. Li, X. G. Yi, X. L. Liu, D. L. Zhao, Y. P. Zhao, and Y. C. Wang, "All-optical analog comparator," Sci. Rep. **6**, 31903 (2016).
8. P. Li, L. X. Sang, D. L. Zhao, Y. L. Fan, K. A. Shore, Y. C. Wang, and A. B. Wang, "All-optical comparator with a step-like transfer function," J. Lightwave Technol. **35**, 5034 (2017).
9. P. P. Ho, Q. Z. Wang, J. Chen, Q. D. Liu, and R. R. Alfano, "Ultrafast optical pulse digitization with unary spectrally encoded cross-phase modulation," Appl. Opt. **36**, 3425 (1997).
10. S. Oda and A. Maruta, "Two-bit all-optical analog-to-digital conversion by filtering broadened and split spectrum induced by soliton effect or self-phase modulation in fiber," IEEE J. Sel. Top. Quantum Electron. **12**, 307 (2006).
11. T. Konishi, K. Tanimura, K. Asano, Y. Oshita, and Y. Ichioka, "All-optical analog-to-digital converter by use of self-frequency shifting in fiber and a pulse-shaping technique," J. Opt. Soc. Am. B **19**, 2817 (2002).
12. C. Xu and X. Liu, "Photonic analog-to-digital converter using soliton self-frequency shift and interleaving spectral filters," Opt. Lett. **28**, 986 (2003).
13. K. Ikeda, J. M. Abdul, S. Namiki, and K. Kitayama, "Optical quantizing and coding for ultrafast A/D conversion using nonlinear fiber-optic switches based on Sagnac interferometer," Opt. Express **13**, 4296 (2005).
14. S. Oda, S. Okamoto, and A. Maruta, "A novel quantization scheme by slicing supercontinuum spectrum for all-optical analog-to-digital conversion," IEEE Photon. Technol. Lett. **17**, 465 (2005).
15. R. Pant, C. Xiong, S. Madden, B. L. Davies, and B. J. Eggleton, "Investigation of all-optical analog-to-digital quantization using a chalcogenide waveguide: a step towards on-chip analog-to-digital conversion," Opt. Commun. **283**, 2258 (2010).
16. S. Kang, J. H. Yuan, Z. Kang, X. T. Zhang, X. Kang, Z. Guo, F. Li, B. B. Yan, K. R. Wang, and X. Z. Sang, "All-optical quantization scheme by slicing the supercontinuum in a chalcogenide horizontal slot waveguide," J. Opt. **17**, 085502 (2015).
17. R. Ma, S. P. Jing, K. R. Wang, J. H. Yuan, C. Mei, T. G. Zhao, B. B. Yan, X. Z. Sang, and C. X. Yu, "Experimental demonstration of all-optical

quantization by slicing the supercontinuum," Opt. Commun. **454**, 124506 (2020).
18. Y. Li, K. Zhu, Z. Kang, W. L. Ho, R. Davidson, C. Lu, B. E. Little, and S. T. Chu, "CMOS-compatible high-index doped silica waveguide with an embedded silicon-nanocrystal strip for all-optical analog-to digital conversion," Photon. Res. **7**, 1200 (2019).
19. M. R. E. Lamont, B. Luther-Davies, D. Y. Choi, S. Madden, and B. J. Eggleton, "Supercontinuum generation in dispersion engineered highly nonlinear ($\gamma =$ 10/W/m) As_2S_3 chalcogenide planar waveguide," Opt. Express **16**, 14938 (2008).
20. Z. Kang, J. H. Yuan, X. T. Zhang, X. Z. Sang, K. R. Wang, Q. Wu, B. B. Yan, F. Li, X. Zhou, K. P. Zhong, G. Y. Zhou, C. X. Yu, G. Farrell, C. Lu, H. Y. Tam, and P. K. A. Wai, "On-chip integratable all-optical quantizer using strong cross-phase modulation in a silicon-organic hybrid slot waveguide," Sci. Rep. **6**, 19528 (2016).
21. T. Nishitani, T. Konishi, and K. Itoh, "Resolution improvement of all-optical analog-to-digital conversion employing self-frequency shift and self-phase-modulation-induced spectral compression," IEEE J. Sel. Top. Quantum Electron. **14**, 724 (2008).
22. C. S. Langhorst and H. G. Webern, "Optical sampling techniques," J. Opt. Fiber Commun. Rep. **2**, 86 (2005).
23. K. Ioakeimidi, R. F. Leheny, S. Gradinaru, P. R. Bolton, R. Aldana, K. Ma, J. E. Clendenin, J. S. Harris, and R. F. W. Pease, "Photoelectronic analog-to-digital conversion: sampling and quantizing at 100 Gs/s," IEEE Trans. Microwave Theory Tech. **53**, 336 (2005).